

The oncolytic peptide LTX-315 triggers necrotic cell death

Sabrina Forveille^{1,2,3,4,†}, Heng Zhou^{1,2,3,4,5,†}, Allan Sauvat^{1,2,3,4}, Lucillia Bezu^{1,2,3,4,5}, Kevin Müller^{1,2,3,4,5}, Peng Liu^{1,2,3,4,5}, Laurence Zitvogel^{5,6,7,8}, Gérard Pierron⁹, Øystein Rekdal^{10,11}, Oliver Kepp^{1,2,3,4,*}, and Guido Kroemer^{1,2,3,4,12,13,*}

¹Metabolomics and Cell Biology Platforms; Gustave Roussy Comprehensive Cancer Institute; Villejuif, France; ²Equipe 11 labellisée Ligue contre le Cancer; Center de Recherche des Cordeliers; INSERM U 1138; Paris, France; ³Université Paris Descartes; Sorbonne Paris Cité; Paris, France; ⁴Université Pierre et Marie Curie; Paris, France; ⁵University of Paris Sud XI; Kremlin Bicêtre, France; ⁶Department of Immuno-Oncology; Institut de Cancérologie Gustave Roussy Cancer Campus; Villejuif, France; ⁷Institut National de la Santé et de la Recherche Médicale (INSERM), U1015; Villejuif, France; ⁸Center of Clinical Investigations in Biotherapies of Cancer (CICBT) 507; Villejuif, France; ⁹Gustave Roussy Comprehensive Cancer Center; Villejuif, France CNRS; UMR8122, Villejuif, France; ¹⁰University of Tromsø; Institute of Medical Biology; Tromsø, Norway; ¹¹Lytx Biopharma; Oslo, Norway; ¹²Pôle de Biologie; Hôpital Européen Georges Pompidou; AP-HP; Paris, France; ¹³Karolinska Institute; Department of Women's and Children's Health; Karolinska University Hospital; Stockholm, Sweden

[†]These authors contributed equally to this work.

Keywords: anticancer immunity, apoptosis, necrosis, LTX-315

The oncolytic peptide LTX-315 has been designed for killing human cancer cells and turned out to stimulate anti-cancer immune responses when locally injected into tumors established in immunocompetent mice. Here, we investigated the question whether LTX-315 induces apoptosis or necrosis. Transmission electron microscopy or morphometric analysis of chromatin-stained tumor cells revealed that LTX-315 failed to induce apoptotic nuclear condensation and rather induced a necrotic phenotype. Accordingly, LTX-315 failed to stimulate the activation of caspase-3, and inhibition of caspases by means of Z-VAD-fmk was unable to reduce cell killing by LTX-315. In addition, 2 prominent inhibitors of regulated necrosis (necroptosis), namely, necrostatin-1 and cyclosporin A, failed to reduce LTX-315-induced cell death. In conclusion, it appears that LTX-315 triggers unregulated necrosis, which may contribute to its pro-inflammatory and pro-immune effects.

Introduction

Antimicrobial peptides typically have a cationic amphiphilic structure in which hydrophobic and positive charged amino acids are located on opposite surfaces. Several *de novo* designed antimicrobial peptide have been based on a sequence motif resembling the peptide KLAKLAK (K = lysine, L = leucine, A = alanine).¹ Such peptides can be fused with plasma membrane transducing domains² and targeted to specific tumor cell antigens^{3–6} the tumor-associated endothelium⁷ or white adipose cells⁸ with the scope of generating agents that selectively ablate specific cell types *in vivo*, upon their systemic administration. Such peptides have been reported to induce apoptosis due to their capacity to induce mitochondrial membrane permeabilization, followed by the release of cytochrome *c* and activation of caspases.^{3–11}

Recently, an optimized antimicrobial peptide, LTX-315 has been designed based on the structure of bovine lactoferricin, which is one of the most studied antimicrobial peptides.¹² LTX-315 has the particularity to cause the regression of B16 melanomas *in vivo* when it is administered into the tumor.^{12,13} This effect involves infiltration of the tumor by T lymphocytes and the stimulation of an anticancer immune response that protects immunocompetent mice cured from

melanoma against subsequent rechallenge with B16 cells.¹² Based on these observations, it has been suggested that LTX-315 may induce immunogenic cell death,^{12,13} a type of cell death that is able to improve the efficacy of anticancer therapies.^{14–24}

Intrigued by these findings, we wondered which particular cell death modality would be induced by LTX-315, knowing that there is a constant debate on the question whether apoptosis or necrosis would constitute a more immunogenic type of cellular demise.^{15,25,26} Here, we report that LTX-315 fails to activate caspases and causes classical necrosis that is refractory to necroptosis inhibitors including necrostatin-1 and cyclosporin A. We also present ultrastructural evidence in favor of the hypothesis that LTX-315 induces a necrotic cell death phenotype.

Results and Discussion

Failure of LTX-315 to induce hallmarks of apoptosis

The major morphological and biochemical hallmarks of apoptosis are nuclear condensation (pyknosis) with fragmentation (karyorrhexis) and the activation of effector caspases, in particular caspase-3.^{27–29} Transmission electron microscopic observation of

*Correspondence to: Oliver Kepp; Email: captain.olsen@gmail.com, Guido Kroemer; Email: kroemer@orange.fr

Submitted: 07/31/2015; Revised: 08/31/2015; Accepted: 09/07/2015

<http://dx.doi.org/10.1080/15384101.2015.1093710>

U2OS osteosarcoma cells treated with LTX-315 (6 h) did not reveal any morphological signs of nuclear apoptosis since nuclei appeared largely intact and major chromatin condensation was absent (Fig. 1). At low concentrations of LTX-315 (12.5 to 50 $\mu\text{g/ml}$), which do not cause immediate cell death defined by plasma membrane permeabilization (see below), the only major morphological change consisted in the dilatation of mitochondria that often manifested a hollow appearance. At higher concentrations (100 $\mu\text{g/ml}$), the vast majority of cells adopted a necrotic morphology with absent plasma membranes and vacuolated cytoplasm. Frequently, cellular remnants remained attached to the culture substrate while manifesting a 'ghost'-like appearance (Fig. 1).

We further analyzed the capacity of LTX-315 to induce chromatin condensation by means of fluorescence microscopy after Hoechst 33342 staining. This method was combined with the detection of activated, proteolytically mature caspase-3 (Casp3a) by immunofluorescence staining of fixed and permeabilized cells.³⁰ The positive control, the pan-tyrosine kinase inhibitor staurosporine, induced a significant degree of caspase-3 activation (detectable as a positive immunofluorescence signal) and nuclear shrinkage (detectable by morphometric analysis of the surface area of the Hoechst 33342 staining). As an additional control, the pan-caspase inhibitor

Z-VAD abolished the activation of caspase-3 and reduced chromatin condensation induced by staurosporine and the uncoupling agent CCCP while necrostatin-1, an inhibitor of the RIP1 kinase,³¹ did not interfere with these parameters (Fig. 2). In contrast, LTX-315 failed to induce both signs of apoptosis (Fig. 2). This result was obtained over a range of LTX-315 concentrations (from 12.5 to 200 $\mu\text{g/ml}$) and at several time points (6 h, 24 h). Hence, LTX-315 is unable to induce the major morphological and biochemical signs of apoptosis.

LTX-315-induced cell death is not affected by major inhibitors of apoptosis and necrosis

In the next step, we stained LTX-315-treated cells with a combination of the vital dye propidium iodide (PI, which is usually excluded from live cells, yet incorporates into necrotic cells via the permeabilized plasma membrane) and Hoechst 33342 (which incorporated into both live and dead cells, although the intensity of the staining tends to increase with cell death). At concentrations of 100–200 $\mu\text{g/ml}$, LTX-315 caused rapid (6 h) cell death as indicated by the PI-detectable loss of plasma membrane integrity. While low concentrations (12.5–25 $\mu\text{g/ml}$) did not affect cellular viability even upon protracted culture (24 h), the intermediate concentration (50 $\mu\text{g/ml}$) caused a mixed phenotype in which half of the cells were dead by 6 h (while half remained viable) and some cells were still alive at 24 h (Fig. 3). These results indicate that the dose response of cell death induction has been fully covered from absent through partial until complete cytotoxicity of LTX-315. Over this dose response range, Z-VAD-fmk failed to prevent cell killing induced by LTX-315. Moreover, necrostatin-1 was unable to interfere with the loss of viability induced by LTX-315 although it did have a partial, significant cytoprotective effect on staurosporine-induced cell loss (detectable at 3 μM staurosporine at 6 h and at 0.3, 1 and 3 μM staurosporine at 24 h) (Fig. 3). Similarly, cyclosporine A, an inhibitor of mitochondrial permeability transition that can prevent some instances of regulated necrosis,^{32,33} failed to interfere with LTX-315-induced cell death (Fig. 4). Images obtained from videomicroscopic studies underline the cytotoxicity of LTX-315 that manifests with cellular disintegration and morphological traits of

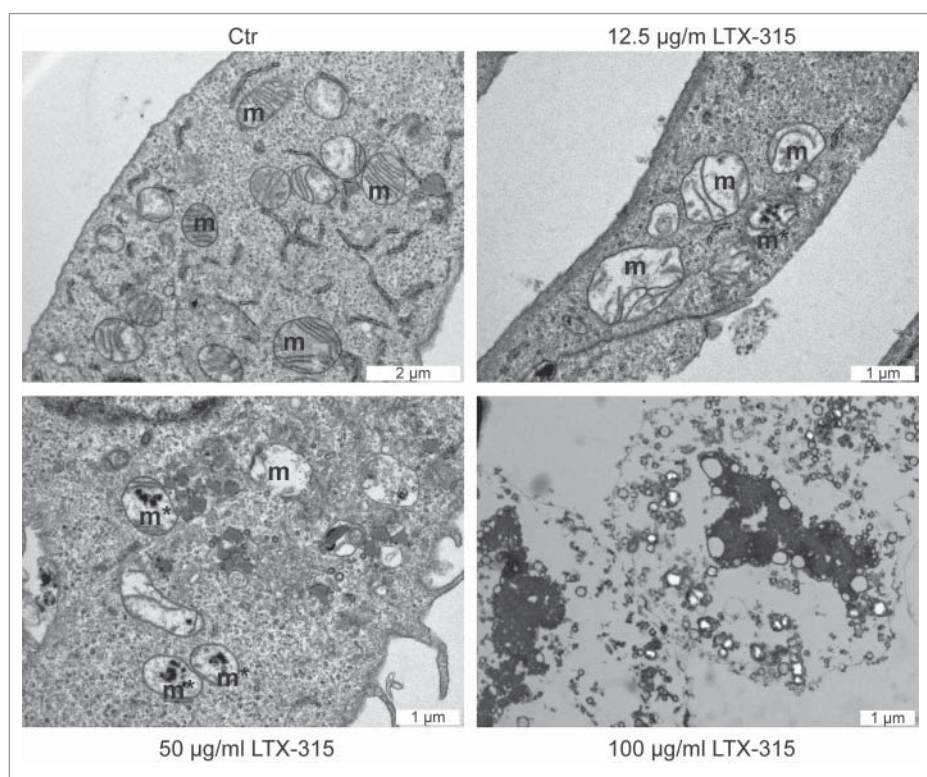


Figure 1. Ultrastructural characteristics of LTX-315-induced cell death. U2OS cells were either left untreated (control, Ctr) or treated with the indicated dose of LTX-315 for 6 hours followed by osmium tetroxide staining and transmission electron microscopy. Note the presence of dilated mitochondria in cells treated with 12.5 or 50 $\mu\text{g/ml}$ of LTX-315.

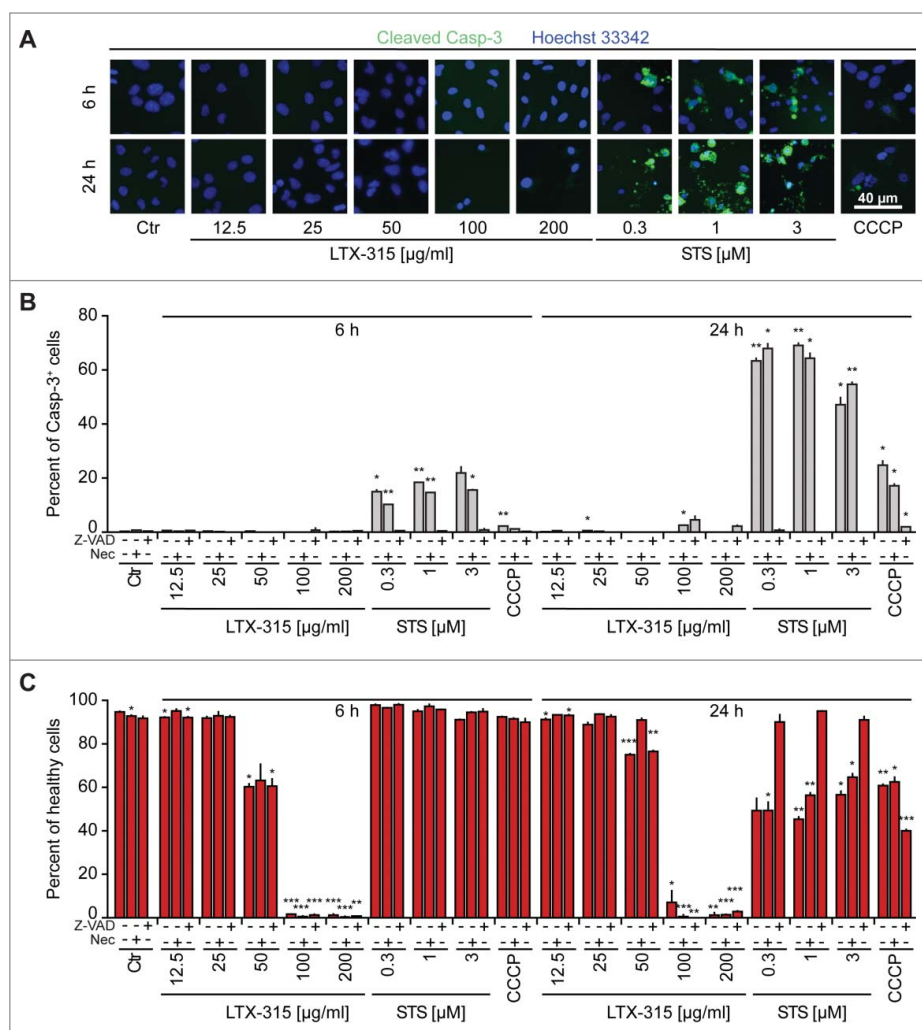


Figure 2. Failure of LTX-315 to induce caspase-3 activation and nuclear shrinkage. U2OS cells were treated for the indicated period with LTX-315, staurosporine (STS) or 100 μ M carbonyl cyanide m-chlorophenyl hydrazine (CCCP) in the absence or presence of the pan-caspase inhibitor Z-VAD or the necroptosis inhibitor necrostatin-1 (Nec), followed by fixation and permeabilization of the cells, immunofluorescence staining for the detection of active caspase 3 (Casp3a) and counterstained with the chromatin dye Hoechst 33342. Representative images are shown in A (images obtained in the absence of Z-VAD and Nec). Quantitative results (means \pm SD of triplicates) are shown in B and C. In B, the frequency of Casp3a⁺ cells is shown for each treatment, while in C, the frequency of cells with normal morphology (not shrunken) is displayed. Asterisks indicate significant differences (unpaired Student t test) with respect to untreated controls. *p < 0.05; **p < 0.01; ***p < 0.001.

necrosis (Fig. 5). Altogether these results indicate that LTX-315 mediated cytotoxic effects do not involve any of the major biochemical pathways associated with regulated necrosis.

Concluding remarks

At differences with other amphipathic cationic peptides designed to

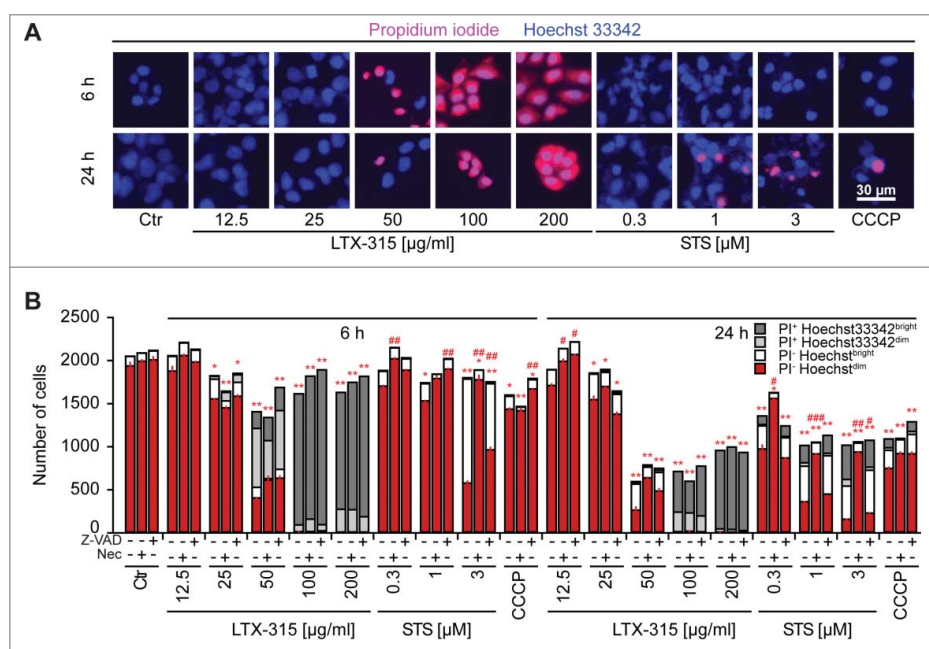


Figure 3. LTX-315-induced cell death is refractory to inhibition by Z-VAD and necrostatin 1. U2OS cells were treated for the indicated period with LTX-315, staurosporine (STS) or 100 μ M carbonyl cyanide m-chlorophenyl hydrazine (CCCP) in the absence or presence of the pan-caspase inhibitor Z-VAD or the necroptosis inhibitor necrostatin-1 (Nec), followed by staining with the vital dye propidium iodide (PI) and the chromatin dye Hoechst 33342. Representative fluorescence microphotographs (images obtained in the absence of Z-VAD and Nec) are shown in A, and quantitative results are shown in B. Asterisks indicate significant differences (unpaired Student t test) in Hoechst^{dim} PI⁺ cell number with respect to untreated controls, for a given co-treatment. *p < 0.05; **p < 0.01; ***p < 0.001. Sharps indicate significant differences, for a given drug treatment, compared to control without co-treatment. #p < 0.05; ##p < 0.01.

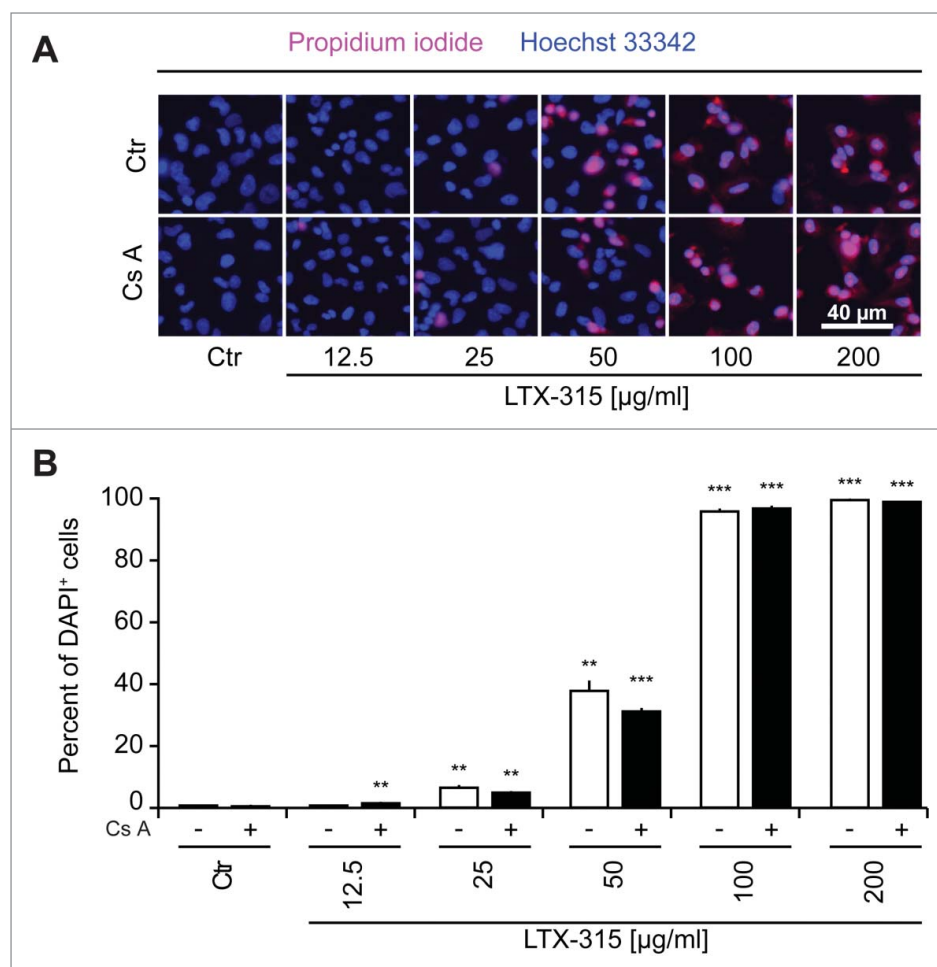


Figure 4. Failure of cyclosporine A to inhibit LTX-315-induced cell death. U2OS cells were treated for 6 hrs with LTX-315 in the absence or presence of 100 nM of the mitochondrial permeability transition inhibitor cyclosporine A (CsA), followed by staining with the vital dye propidium iodide (PI) and the chromatin dye Hoechst 33342. Representative fluorescence microphotographs are shown in **A**, and quantitative results are shown in **B**. Asterisks indicate significant differences (unpaired Student t test) in Hoechst^{dim} PI⁺ cell number with respect to untreated controls, for a given co-treatment. * $p < 0.05$; ** $p < 0.01$; *** $p < 0.001$.

kill cells,³⁻⁸ LTX-315 fails to activate caspases through the intrinsic (mitochondrial) pathway and hence fails to activate classical apoptosis. Rather, LTX-315 appears to activate a direct pro-necrotic pathway that, however, is neither inhibited by necrostatin-1 nor by cyclosporine A. LTX-315-induced necrosis was preceded by major changes in mitochondrial morphology, as this may be expected from this kind of agent, and then culminated in rapid disintegration of the plasma membrane, vacuolization of the cytoplasmic remnant and ghost-like appearance of the nucleus, which failed to exhibit consistent signs of chromatin condensation. LTX-315 has recently been shown to act on mitochondrial membranes to cause cell death.³⁴ This fact may explain why LTX-315 has a relatively low toxicity on cells lacking mitochondria, such as erythrocytes.³⁴ Moreover, the intrinsic aberration of mitochondrial function in cancer cells may predispose them to the cytotoxic action of

LTX-315,^{35,36} a possibility that is currently explored in a phase I clinical trial in Europe. Given the particular capacity of LTX-315 to stimulate an anticancer immune response if injected locally into melanomas implanted in immunocompetent, haploidentical hosts,^{12,13} it is tempting to speculate, yet remains to be demonstrated, that LTX-315 is inducing a new modality of immunogenic cell death. Hence, the capacity of LTX-315 to lyse tumor cells in a non-physiological (and unconventional) fashion might contribute to its pro-immune effects. Further studies are required to understand the particular mechanisms through which LTX-315 achieves these properties and which danger-associated molecules are liberated by LTX-315 to provoke local inflammation and immune reactions in tissues.

Materials & Methods

Chemicals and cell cultures

Media and supplements for cell culture were obtained from Gibco-Life Technologies (Carlsbad, CA, USA), chemicals from Sigma-Aldrich (St. Louis, MO, USA) with the exception of LTX-315 that was provided by Lytix Biopharma (Tromsø, Norway); Z-VAD FMK from Bachem (Bubendorf, Switzerland), Hoechst 33342, DAPI, DIOC₆(3), and plastic ware from Greiner Bio-One (Monroe, CA, USA). Primary antibodies (cleaved caspase-3; #9661) were purchased from Cell Signaling (Danvers, MA; USA) and secondary Alexa Fluor-labeled antibodies came from Life Technologies. Human osteosarcoma U2OS cells were cultured in Glutamax[®]-containing DMEM medium supplemented with 10% fetal calf serum (FCS), and 10 mM HEPES buffer. Cells were grown at 37°C in a humidified incubator under a 5% CO₂ atmosphere.

High-throughput assessment of cell death

Five $\times 10^3$ U2OS cells were seeded into black 96-well μclear imaging plates (Greiner Bio-One) and allowed to adapt for 24 hrs. Thereafter the cells were treated with the LTX-315 compounds and respective controls and incubated for additional 6 or 24 hrs before either 1 μM of DAPI or a mixture 1 μM Hoechst and 1 μM propidium iodide were

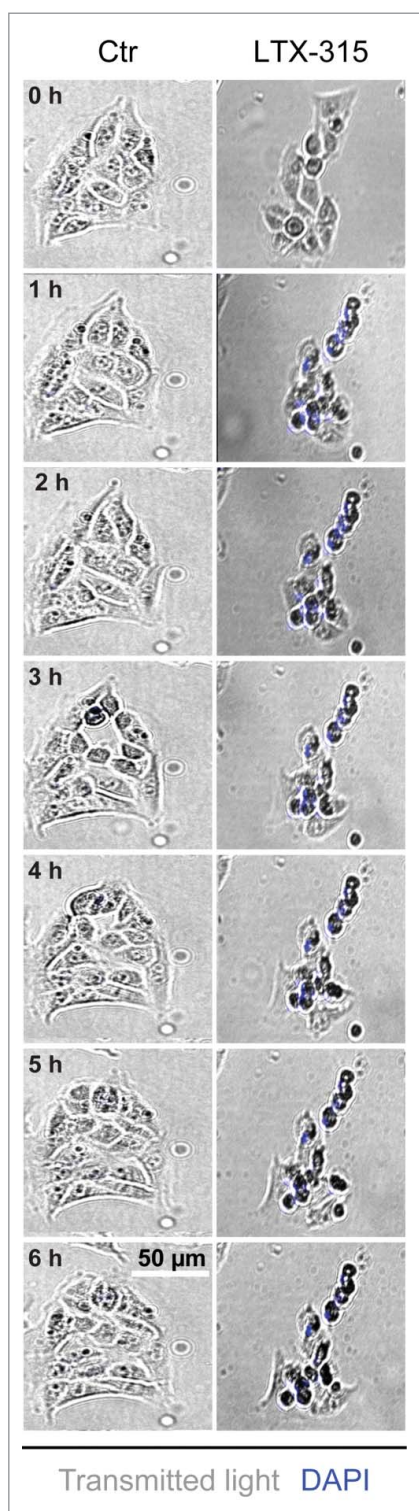


Figure 5. Videomicroscopy of cellular disintegration. U2OS cells were treated for the indicated period with LTX-315 in the presence of 1 μ M DAPI. Morphological changes and the uptake of the exclusion dye were monitored by videomicroscopy. Representative image galleries from U2OS cells treated with 50 μ g/ml LTX-315 or left untreated are depicted.

added upon treatment immediately before monitoring the uptake of the exclusion dye in a minimum of 4 view fields per well by means of an ImageXpress micro XL automated bioimager (Molecular Devices) equipped with a PlanApo 20X/0.75 NA objective (Nikon).

Live cell imaging

Five $\times 10^3$ U2OS cells were seeded into black 96-well μ clear imaging plates (Greiner Bio-One) and allowed to adapt for 24 hrs. Thereafter the cells were treated with LTX-315 and respective controls and DAPI was added at a final concentration of 1 μ M. The cells were placed in an ImageXpress micro XL automated bioimager (Molecular Devices) equipped with an environmental control unit and an IBIDI gas mixer (Munich, Germany) providing 37°C and 5% CO₂ humidified atmosphere. A minimum of 4 view fields per well were acquired using transmitted light and DAPI filters with a PlanApo 20X/0.75 NA objective (Nikon).

Immunostaining

Five $\times 10^3$ U2OS cells were seeded into black 96-well μ clear imaging plates (Greiner Bio-One) and allowed to adapt for 24 hrs. Thereafter the cells were treated with LTX-315 compounds and respective controls and incubated for additional 6 or 24 hrs before fixation in 3.7 % (w/v) paraformaldehyde in PBS supplemented with 1 μ M Hoechst 33342 for 20 min.³⁷⁻³⁹ Upon fixation cells were permeabilized with 0.1 % Triton in PBS for 10min at RT. Unspecific binding was blocked with 2 % BSA in PBS for 10 min at RT followed by primary antibody diluted in BSA 2 % following the manufactures recommendations over night on shaker at 4°C. The cells were rinsed twice and stained with AlexaFluor-coupled secondary antibodies for 1 h at RT, rinsed twice and subjected to imaging using an ImageXpress micro XL automated bioimager (Molecular Devices) equipped with a PlanApo 20X/0.75 NA objective (Nikon).

Transmission electron microscopy

For ultrastructural studies, human osteosarcoma U2OS cells were fixed in 1.6 % glutaraldehyde (v/v in 0.1 M phosphate buffer) for 1 h, collected by scraping, centrifuged and the pellet was post-fixed 1 % osmium tetroxide (w/v in 0.1 M phosphate buffer). Following dehydration through a graded ethanol series, cells were embedded in EponTM 812 and ultrathin sections were stained with standard uranyl acetate and lead citrate. Images were taken using a Tecnai 12 electron microscope (FEL, Eindhoven, the Netherlands).

Data processing and statistical analyses

Unless otherwise specified, experiments were performed in triplicate parallel instances and repeated at least once, and data were analyzed with the R software (<http://www.r-project.org/>). Microscopy images were segmented and analyzed by means of the MetaXpress (Molecular Devices) software and numerical data was further processed with R. Unless otherwise specified, data are presented as means \pm SD. Thresholds for the minimum number of events in each analysis necessary to apply further statistics were

calculated based on a medium effect size (according to Cohen's conventional criteria) using the *pwr* package for R with a targeted value of 0.95. Samples that did not match the requirements were marked ND and were excluded from the analysis.

Disclosure of Potential Conflicts of Interest

No potential conflicts of interest were disclosed.

Funding

HZ and PL are supported by the China Scholarship Council. GK and LZ are supported by the Ligue contre le Cancer (équipes labélisées); Agence National de la Recherche (ANR) – Projets

blancs; ANR under the frame of E-Rare-2, the ERA-Net for Research on Rare Diseases; Association pour la recherche sur le cancer (ARC); Cancéropôle Ile-de-France; Institut National du Cancer (INCa); Fondation Bettencourt-Schueller; Fondation de France; Fondation pour la Recherche Médicale (FRM); the European Commission (ArtForce); the European Research Council (ERC); the LabEx Immuno-Oncology; the SIRIC Stratified Oncology Cell DNA Repair and Tumor Immune Elimination (SOCRATE); the SIRIC Cancer Research and Personalized Medicine (CARPEM); the Swiss Bridge Foundation, ISREC and the Paris Alliance of Cancer Research Institutes (PACRI). This project was supported by Lytix Biopharma Ltd.

References

- Javadpour MM, Juban MM, Lo WC, Bishop SM, Alberty JB, Cowell SM, Becker CL, McLaughlin ML. De novo antimicrobial peptides with low mammalian cell toxicity. *J Med Chem* 1996; 39:3107-13; PMID:8759631; <http://dx.doi.org/10.1021/jm9509410>
- Mai JC, Mi Z, Kim SH, Ng B, Robbins PD. A proapoptotic peptide for the treatment of solid tumors. *Cancer Res* 2001; 61:7709-12; PMID:11691780
- Ellerby HM, Arap W, Ellerby LM, Kain R, Andrusiak R, Rio GD, Krajewski S, Lombardo CR, Rao R, Ruoslahti E, et al. Anti-cancer activity of targeted pro-apoptotic peptides. *Nat Med* 1999; 5:1032-8; PMID:10470080; <http://dx.doi.org/10.1038/12469>
- Kelly KA, Jones DA. Isolation of a colon tumor specific binding peptide using phage display selection. *Neoplasia* 2003; 5:437-44; PMID:14670181; [http://dx.doi.org/10.1016/S1476-5586\(03\)80046-5](http://dx.doi.org/10.1016/S1476-5586(03)80046-5)
- Marks AJ, Cooper MS, Anderson RJ, Orchard KH, Hale G, North JM, Ganeshaguru K, Steele AJ, Mehta AB, Lowdell MW, et al. Selective apoptotic killing of malignant hemopoietic cells by antibody-targeted delivery of an amphipathic peptide. *Cancer Res* 2005; 65:2373-7; PMID:15781652; <http://dx.doi.org/10.1158/0008-5472.CAN-04-2594>
- Mandelin J, Cardo-Vila M, Driessen WH, Mathew P, Navone NM, Lin SH, Logothetis CJ, Rietz AC, Dobr-off AS, Proneth B, et al. Selection and identification of ligand peptides targeting a model of castrate-resistant osteogenic prostate cancer and their receptors. *Proc Natl Acad Sci U S A* 2015; 112:3776-81; PMID:25762070
- Arap W, Haedicke W, Bernasconi M, Kain R, Rajotte D, Krajewski S, Ellerby HM, Bredesen DE, Pasqualini R, Ruoslahti E. Targeting the prostate for destruction through a vascular address. *Proc Natl Acad Sci U S A* 2002; 99:1527-31; PMID:11830668; <http://dx.doi.org/10.1073/pnas.241655998>
- Barnhart KF, Christianson DR, Hanley PW, Driessen WH, Bernacky BJ, Baze WB, Wen S, Tian M, Ma J, Kolonin MG, et al. A peptidomimetic targeting white fat causes weight loss and improved insulin resistance in obese monkeys. *Sci Transl Med* 2011; 3:108ra12; <http://dx.doi.org/10.1126/scitranslmed.3002621>
- Macho A, Decaudin D, Castedo M, Hirsch T, Susin SA, Zamzami N, Kroemer G. Chloromethyl-X-Rosamine is an aldehyde-fixable potential-sensitive fluorochrome for the detection of early apoptosis. *Cytometry* 1996; 25:333-40; PMID:8946140; [http://dx.doi.org/10.1002\(SICI\)1097-0320\(19961201\)25:4%3c333::AID-CYTO4%3e3.0.CO;2-E](http://dx.doi.org/10.1002(SICI)1097-0320(19961201)25:4%3c333::AID-CYTO4%3e3.0.CO;2-E)
- Metivier D, Dallaporta B, Zamzami N, Larochette N, Susin SA, Marzo I, Kroemer G. Cytofluorometric detection of mitochondrial alterations in early CD95/Fas/APO-1-triggered apoptosis of Jurkat T lymphoma cells. Comparison of seven mitochondrion-specific fluorochromes. *Immunol Lett* 1998; 61:157-63; PMID:9657269; [http://dx.doi.org/10.1016/S0165-2478\(98\)00013-3](http://dx.doi.org/10.1016/S0165-2478(98)00013-3)
- Penning JM, Kroemer G. Mitochondria, AIF and caspases—rivaling for cell death execution. *Nat Cell Biol* 2003; 5:97-9; PMID:12563272; <http://dx.doi.org/10.1038/ncb0203-97>
- Camilio KA, Berge G, Ravuri CS, Rekdal O, Sveinbjornsson B. Complete regression and systemic protective immune responses obtained in B16 melanomas after treatment with LTX-315. *Cancer Immunol Immunother* 2014; 63:601-13; PMID:24676901; <http://dx.doi.org/10.1007/s00262-014-1540-0>
- Camilio KA, Rekdal O, Sveinbjornsson B. LTX-315 (Oncoport): A short synthetic anticancer peptide and novel immunotherapeutic agent. *Oncoimmunology* 2014; 3:e29181; PMID:25083333; <http://dx.doi.org/10.4161/onci.29181>
- Zitvogel L, Galluzzi L, Smyth MJ, Kroemer G. Mechanism of action of conventional and targeted anticancer therapies: reinstating immunosurveillance. *Immunity* 2013; 39:74-88; PMID:23890065; <http://dx.doi.org/10.1016/j.immuni.2013.06.014>
- Kepp O, Senovilla L, Vitale I, Vacchelli E, Adjemian S, Agostinis P, Apetoh L, Aranda F, Barnaba V, Bloy N, et al. Consensus guidelines for the detection of immunogenic cell death. *Oncoimmunology* 2014; 3:e955691
- Golden EB, Frances D, Pellicciotta I, Demaria S, Helen Barcellos-Hoff M, Formenti SC. Radiation fosters dose-dependent and chemotherapy-induced immunogenic cell death. *Oncoimmunology* 2014; 3:e28518; PMID:25071979; <http://dx.doi.org/10.4161/onci.28518>
- Calvet CY, Famin D, Andre FM, Mir LM. Electrochemotherapy with bleomycin induces hallmarks of immunogenic cell death in murine colon cancer cells. *Oncoimmunology* 2014; 3:e28131; PMID:25083316; <http://dx.doi.org/10.4161/onci.28131>
- Sukkurwala AQ, Adjemian S, Senovilla L, Michaud M, Spaggiari S, Vacchelli E, Baracco EE, Galluzzi L, Zitvogel L, Kepp O, et al. Screening of novel immunogenic cell death inducers within the NCI Mechanistic Diversity Set. *Oncoimmunology* 2014; 3:e28473; PMID:25050214; <http://dx.doi.org/10.4161/onci.28473>
- Michaud M, Sukkurwala AQ, Di Sano F, Zitvogel L, Kepp O, Kroemer G. Synthetic induction of immunogenic cell death by genetic stimulation of endoplasmic reticulum stress. *Oncoimmunology* 2014; 3:e28276; PMID:25050202; <http://dx.doi.org/10.4161/onci.28276>
- Tesniere A, Schlemmer F, Boige V, Kepp O, Martins I, Ghiringhelli F, Aymeric L, Michaud M, Apetoh L, Barault L, et al. Immunogenic death of colon cancer cells treated with oxaliplatin. *Oncogene* 2010; 29:482-91; PMID:19881547; <http://dx.doi.org/10.1038/onc.2009.356>
- Pol J, Vacchelli E, Aranda F, Castoldi F, Eggermont A, Cremer I, Sautès-Fridman C, Fucikova J, Galon J, Spisek R, et al. Trial Watch: Immunogenic cell death inducers for anticancer chemotherapy. *Oncoimmunology* 2015; 4:e1008866; PMID:26137404; <http://dx.doi.org/10.1080/2162402X.2015.1008866>
- Bloy N, Pol J, Manic G, Vitale I, Eggermont A, Galon J, Tartour E, Zitvogel L, Kroemer G, Galluzzi L. Trial Watch: Radioimmunotherapy for oncological indications. *Oncoimmunology* 2014; 3:e954929; PMID:25941606; <http://dx.doi.org/10.4161/21624011.2014.954929>
- Vacchelli E, Aranda F, Eggermont A, Galon J, Sautès-Fridman C, Cremer I, Zitvogel L, Kroemer G, Galluzzi L. Trial Watch: Chemotherapy with immunogenic cell death inducers. *Oncoimmunology* 2014; 3:e27878; PMID:24800173; <http://dx.doi.org/10.4161/onci.27878>
- Ma Y, Adjemian S, Galluzzi L, Zitvogel L, Kroemer G. Chemokines and chemokine receptors required for optimal responses to anticancer chemotherapy. *Oncoimmunology* 2014; 3:e27663; PMID:24800170; <http://dx.doi.org/10.4161/onci.27663>
- Green DR, Ferguson T, Zitvogel L, Kroemer G. Immunogenic and tolerogenic cell death. *Nat Rev Immunol* 2009; 9:353-63; PMID:19365408; <http://dx.doi.org/10.1038/nri2545>
- Werthmoller N, Frey B, Wunderlich R, Fietkau R, Gaipal US. Modulation of radiochemoimmunotherapy-induced B16 melanoma cell death by the pan-caspase inhibitor zVAD-fmk induces anti-tumor immunity in a HMGB1-, nucleotide- and T-cell-dependent manner. *Cell Death Dis* 2015; 6:e1761; PMID:25973681; <http://dx.doi.org/10.1038/cddis.2015.129>
- Galluzzi L, Vitale I, Abrams JM, Alnemri ES, Baehrecke EH, Blagosklonny MV, Dawson TM, Dawson VL, El-Deiry WS, Fulda S, et al. Molecular definitions of cell death subroutines: recommendations of the Nomenclature Committee on Cell Death 2012. *Cell Death Differ* 2012; 19:107-20; PMID:21760595; <http://dx.doi.org/10.1038/cdd.2011.96>
- Galluzzi L, Bravo-San Pedro JM, Vitale I, Aaronson SA, Abrams JM, Adam D, Alnemri ES, Altucci L, Andrews D, Annicchiarico-Petruzzelli M, et al. Essential versus accessory aspects of cell death: recommendations of the NCCD 2015. *Cell Death Differ* 2015; 22:58-73; PMID:25236395; <http://dx.doi.org/10.1038/cdd.2014.137>
- Tailler M, Senovilla L, Lainey E, Thepot S, Metivier D, Sebert M, Baud V, Billot K, Fenaux P, Galluzzi L, et al. Antineoplastic activity of ouabain and pyriithione zinc in acute myeloid leukemia. *Oncogene* 2012; 31:3536-46; PMID:22105358; <http://dx.doi.org/10.1038/onc.2011.521>
- Kepp O, Galluzzi L, Lipinski M, Yuan J, Kroemer G. Cell death assays for drug discovery. *Nat Rev Drug Discov* 2011; 10:221-37; PMID:21358741; <http://dx.doi.org/10.1038/nrd3373>
- Degterev A, Huang Z, Boyce M, Li Y, Jagtap P, Mizushima N, Cuny GD, Mitchison TJ, Moskowitz

- MA, Yuan J. Chemical inhibitor of nonapoptotic cell death with therapeutic potential for ischemic brain injury. *Nat Chem Biol* 2005; 1:112-9; PMID:16408008; <http://dx.doi.org/10.1038/nchembio711>
32. Linkermann A, Green DR. Necroptosis. *N Engl J Med* 2014; 370:455-65; PMID:24476434; <http://dx.doi.org/10.1056/NEJMra1310050>
33. Green DR, Galluzzi L, Kroemer G. Cell biology. Metabolic control of cell death. *Science* 2014; 345:1250256; PMID:25237106; <http://dx.doi.org/10.1126/science.1250256>
34. Zhou H, Forveille S, Sica V, Izzo V, Durand S, Müller K, Liu P, Zitvogel L, Rekdal Ø, Kepp O, et al. The oncolytic peptide LTX-315 kills cancer cells through Bax/Bak-regulated mitochondrial membrane permeabilization. *Oncotarget* 2015; 6 (29):26599-614
35. Galluzzi L, Kepp O, Kroemer G. Mitochondria: master regulators of danger signalling. *Nat Rev Mol Cell Biol* 2012; 13:780-8; PMID:23175281; <http://dx.doi.org/10.1038/nrm3479>
36. Galluzzi L, Kepp O, Vander Heiden MG, Kroemer G. Metabolic targets for cancer therapy. *Nat Rev Drug Discov* 2013; 12:829-46; PMID:24113830; <http://dx.doi.org/10.1038/nrd4145>
37. Galluzzi L, Morselli E, Vitale I, Kepp O, Senovilla L, Criollo A, Servant N, Paccard C, Hupé P, Robert T, et al. miR-181a and miR-630 regulate cisplatin-induced cancer cell death. *Cancer Res* 2010; 70:1793-803; PMID:20145152; <http://dx.doi.org/10.1158/0008-5472.CAN-09-3112>
38. Michels J, Vitale I, Galluzzi L, Adam J, Olausen KA, Kepp O, Senovilla L, Talhaoui I, Guegan J, Enot DP, et al. Cisplatin resistance associated with PARP hyperactivation. *Cancer Res* 2013; 73:2271-80; PMID:23554447; <http://dx.doi.org/10.1158/0008-5472.CAN-12-3000>
39. Ma Y, Mattarollo SR, Adjemian S, Yang H, Aymeric L, Hannani D, Portela Catani JP, Duret H, Teng MW, Kepp O, et al. CCL2/CCR2-dependent recruitment of functional antigen-presenting cells into tumors upon chemotherapy. *Cancer Res* 2014; 74:436-45; PMID:24302580; <http://dx.doi.org/10.1158/0008-5472.CAN-13-1265>